

When Pretty Isn't Useful: Investigating Why Modern Text-to-Image Models Fail as Reliable Training Data Generators

Krzysztof Adamkiewicz^{1,2†} Brian Moser^{2†} Stanislav Frolov^{2†}
Tobias Christian Nauen^{1,2} Federico Raue² Andreas Dengel^{1,2}

¹RPTU University Kaiserslautern-Landau, Kaiserslautern, Germany

²German Research Center for Artificial Intelligence (DFKI), Kaiserslautern, Germany

[†]Equal contribution

first.last@dfki.de first.second.last@dfki.de

Abstract

Recent text-to-image (T2I) diffusion models produce visually stunning images and demonstrate excellent prompt following. But do they perform well as synthetic vision data generators? In this work, we revisit the promise of synthetic data as a scalable substitute for real training sets and uncover a surprising performance regression. We generate large-scale synthetic datasets using state-of-the-art T2I models released between 2022 and 2025, train standard classifiers solely on this synthetic data, and evaluate them on real test data. Despite observable advances in visual fidelity and prompt adherence, classification accuracy on real test data consistently declines with newer T2I models as training data generators. Our analysis reveals a hidden trend: These models collapse to a narrow, aesthetic-centric distribution that undermines diversity and real data distribution coverage. Overall, our findings challenge a growing assumption in vision research, namely that progress in generative realism implies progress in data realism. We thus highlight an urgent need to rethink the capabilities of modern T2I models as reliable training data generators.

1. Introduction

Quality, quantity, and distribution of training data are fundamental determinants of performance and generalization in modern deep learning [8, 24, 25, 40, 54]. Yet as model architectures grow in scale and capacity, their appetite for vast, diverse, and well-curated data has rapidly outpaced the availability of real-world datasets [20, 37, 42]. Collecting, annotating, and balancing such data has become an increasingly prohibitive bottleneck, particularly in domains constrained by privacy, limited sample availability, or strong domain shifts [3, 7, 19, 27, 58]. As a result, data scarcity,

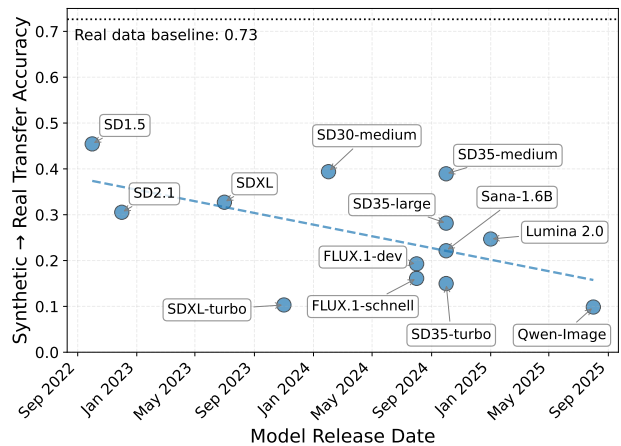


Figure 1. We train ResNet-50 classifiers on images generated by various T2I models for a subset of ImageNet-1k classes and evaluate their accuracy on real test data (Synth → Real). Our results reveal a downward trend over time. Newer models get progressively worse as reliable training data generators.

not model capacity, is often the limiting factor in scaling.

Recent progress in text-to-image (T2I) diffusion has been seen as a promising way to overcome this bottleneck. Modern systems such as Stable Diffusion [11, 38, 43], Flux [28], and Qwen-Image [57] can now generate detailed and diverse images from text alone. This capability has fueled interest in using synthetic data as a scalable, privacy-preserving, and domain-flexible alternative to real datasets. However, despite these advances in visual quality, it remains unclear whether such progress also improves the *usefulness* of synthetic images for training downstream models.

A growing body of work explores this question across a wide range of vision tasks. For classification, several studies have shown that models trained entirely on syn-

thetic data can approach or even match real-data performance [27, 47, 49, 53, 61]. Similar findings extend to object detection [13, 44, 55, 62], contrastive learning [21, 52], continual learning [26, 34, 48], and human pose estimation [46, 56, 59]. These works demonstrate that, under controlled conditions, synthetic data can rival real data while avoiding the costs and constraints of manual curation.

It seems intuitive that as T2I models improve in fidelity, resolution, and photorealism, the synthetic data they produce should become correspondingly more effective for training. We test this intuition through a large-scale benchmark of thirteen state-of-the-art T2I models released between 2022 and 2025. By evaluating how well classifiers trained solely on synthetic data transfer to real test data in an image recognition task, we examine whether improvements in perceptual quality lead to improved capability as reliable training data generators. Despite rapid progress in visual quality [38, 41] and photorealism [45], most of these works [19, 21, 44, 52, 55] still rely on earlier diffusion models. As a result, the implications of newer advances (*i.e.*, larger networks, internet-scale datasets, higher-resolution latent spaces, and stronger prompt conditioning) remain poorly understood in the context of synthetic data quality. This leads to our central and deceptively simple research question: *Does progress in T2I generation actually translate into better synthetic training data for vision models?*

Our findings surprisingly challenge this expectation of performance improvement. In Figure 1, we show that classification accuracy on real test data consistently declines with newer T2I models as training data generators despite observable advances in visual fidelity and prompts adherence. In this work, we investigate the reasons for this decline by probing texture, structure and spectral frequency mismatches to real data. We find that newer models collapse to narrow, aesthetic-centric distributions that undermine diversity and label alignment. And while using detailed text prompts, such as in [12, 30] can improve the downstream performance on real data, this gain comes at a cost: the synthetic manifolds become increasingly compact (*i.e.*, high in density but low in coverage) signaling distributional drift and reduced intra-class diversity.

Our analysis separates sample realism from distribution realism and investigates several independent aspects of synthetic images showing that modern T2I models, though producing visually impressive images that look better, actually function worse as reliable training data generators. In summary, we make the following key contributions:

- A **large-scale, time-spanning benchmark** of T2I models as training data generators. We evaluate thirteen open-source T2I models (2022-2025) on a controlled ImageNet-1K setup and show that, despite better visual fidelity and prompt following, Synth→Real accuracy decreases for newer models.

- Probing **texture and frequency mismatches**. Using depth-based (structure) classifiers, local BagNet (texture) classifiers, and low/high-pass filtered inputs, we find that global structure and low frequencies are well retained, while texture quality and high-frequency detail are systematically degraded with newer models.
- Measuring **drift and diversity loss** in feature space. By measuring density & coverage as well as comparing Real→Synth vs. Synth→Real transfer, we show that newer T2I models exhibit degraded distributional realism.

2. Related Work

2.1. Text-to-Image Generation

Text-to-image (T2I) generation has advanced rapidly in recent years, largely driven by diffusion-based architectures. Early systems such as Stable Diffusion [43] established latent diffusion as the dominant framework for controllable T2I synthesis. Subsequent versions like SDXL [38] improved sampling efficiency through distillation and introduced higher-resolution latent spaces that enhanced visual fidelity. More recent models, including FLUX [28], Qwen-Image [57], and Lumina Image 2.0 [39], further unify text and image tokenization and refine the diffusion process itself for sharper, more coherent generation. Despite these advances in fidelity and controllability, their effectiveness as generators of *useful training data* remains largely untested.

2.2. Synthetic Vision Data

Tian et al. [52] reported that self-supervised representation learning on synthetic data can match or even surpass real data performance. Similarly, Lomurno et al. [33] showed that class-conditioned and fine-tuned diffusion models can occasionally produce competitive synthetic datasets, though primarily in small-scale, low-resolution domains. In a similar fashion, Hammoud et al. [21] successfully performs large-scale training of a CLIP model on fully synthetic vision-language data but with much lower data efficiency as compared to using real data. On the other hand, Geng et al. [17] systematically compared models trained on synthetic images from Stable Diffusion [43] with those trained on images retrieved from Stable Diffusion’s training dataset. They found that synthetic datasets consistently underperform real ones when evaluated on real test data, aligning with our observations. Our work reveals that the performance gap identified in prior work remains inadequately addressed in the latest state-of-the-art T2I models and while they excel at visual fidelity, they increasingly diverge from the data realism required for effective learning.

2.3. Prompt Engineering for Synthetic Training

A complementary line of work focuses on improving the input *text prompts*. Caption-in-Prompt (CiP) [12, 30] ex-

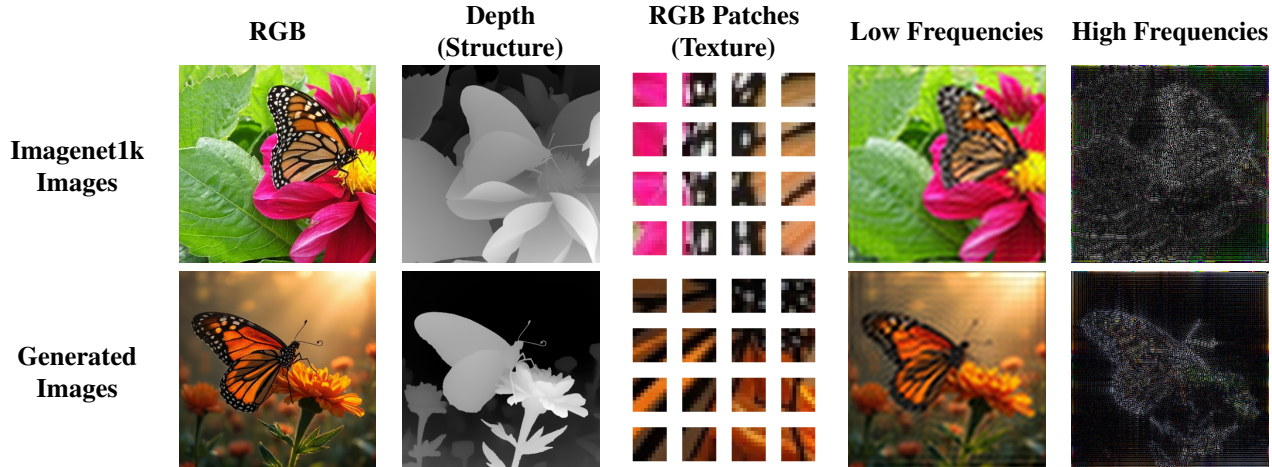


Figure 2. To probe which aspects of synthetic images are most affected, we transform images to suppress or amplify the effects of distortions in a given domain. To separate the effect of low and high level details, we measure the performance gap when training in depth space, which removes textures, and training a low-receptive-field (visualized in the figure) classifier which operates on 9×9 image patches and hence does not rely on structure. To separate the effects of high and low frequency distortions, we train on low and high-pass filtered images. Removing offending features should close the gap with relation to RGB, while removing non-offending features should widen it.

tends class labels with short descriptive captions that add semantic context and enhance object-background separation. Without modifying the generator, this approach consistently improves classifier performance on synthetic images produced by Stable Diffusion models. These studies suggest that richer prompts can partially recover the diversity lost when relying solely on class names. Building on this idea, we also analyze how prompt detail interacts with successive generations of T2I models. Our results show that newer models need very detailed prompts to produce useful training data. Yet even under detailed captioning, texture quality remains limited, and high-frequency detail continues to misalign.

2.4. Dataset Distillation with Generative Priors

Another direction seeks to *learn* synthetic data distributions that are directly optimized for downstream performance. Instead of relying solely on pretrained generators, these methods train compact synthetic datasets under a generative prior to retain the training signal of a large real dataset. Recent approaches such as GLaD [6], LD3M [35], and D⁴M [51] extend dataset distillation into the generative domain by coupling diffusion or adversarial priors with gradient- or feature-level matching. These methods explicitly optimize for *data utility*, often achieving high performance with only a fraction of the original data, albeit at high computational cost. In contrast, our study evaluates *off-the-shelf* T2I models that are optimized for visual realism rather than training utility, showing that generative progress does not automatically translate into useful data for learning. Given their shared reliance on generative priors, we expect similar limi-

tations to emerge in this line of work as well, underscoring the need for learnability-centered evaluation and design.

3. Methodology

Building on prior work [1, 9, 17], we identify three main factors likely responsible for the observed performance gap: (i) texture and structure distortion, (ii) high-frequency distortion, and (iii) distributional drift and diversity collapse.

To isolate their effects, we conduct controlled transformations of the data (Figure 2). For (i), we modify images to either suppress or emphasize texture and structure, respectively. For (ii), we modify images by high- and low-pass filtering. For (iii), we analyze the structural alignment of the synthetic and real data distributions using coverage and density metrics that separately quantify fidelity and diversity.

3.1. Low-Level Texture & High-Level Structure

Previous work by Geng et al. [17] shows that even relatively unnoticeable generator artifacts are strong enough to damage class-relevant details in fine-grained classification tasks. Moreover, convolutional neural networks are known to exhibit a *texture bias* [16], which potentially makes them particularly sensitive to distortions and artifacts at the texture level.

To quantify the contribution of such low-level artifacts, we compare the performance gap of models trained on transformed synthetic and real data in two settings: A model trained to classify solely based on **Structure** and another solely based on **Texture**. The structure classifier is a ResNet-50 operating on depth maps obtained by monocular estimation using the Depth Anything V2 [60] model (see Figure 2:

Depth). The texture classifier is a BagNet [5] classifier which operates on 9×9 image patches (see Figure 2: RGB Patches). Depth space removes all color and textural information, leaving only the overall structures and shapes intact, while the low receptive field of BagNet makes it incapable of seeing beyond textures. Structure models are trained *and* tested in depth space to account for drop due to information removal. If texture artifacts are a key contributor to the observed performance gap, we expect the gap to decrease in the structure-based setting. In the structure-based setting, problematic textures are removed, in contrast to the texture-based setting, where they dominate the signal.

3.2. High-Frequency Distortion

Natural images follow an approximate power-law amplitude spectrum, with energy decaying as a function of spatial frequency f according to $S(f) \propto f^{-\alpha}$ [2, 14]. However, Corvi et al. [9] observed that diffusion-based image generators deviate from this natural distribution, often exhibiting a shift toward high-frequency components. At the same time, CNNs are known to be biased toward high-frequency information [15], making them particularly sensitive to high-frequency spectral distortions.

To quantify the impact of such distortions, we train and evaluate ResNet-50 on high- and low-pass-filtered versions of real and synthetic images (see Figure 2: Low & High Frequencies). The high-pass condition quantifies the performance gap on images that retain frequencies $f \leq 0.2 \times f_N$, while in the low-pass setting images retain $f \geq 0.8 \times f_N$ with f_N referring to the Nyquist frequency.

If the realism of high-frequency components is degraded, we expect the relative performance gap to shrink under low-pass filtering (which removes the mismatched parts of the spectrum) compared to high-pass filtering (which leaves the mismatched spectrum intact).

3.3. Distributional Drift and Diversity Collapse

Prior work has shown that generative models often trade diversity for fidelity, concentrating samples within a limited region of the real data manifold [1, 4, 36, 45]. We hypothesize that this fidelity-diversity trade-off (*i.e.*, greater realism of single samples at the cost of reduced realism of the sample distribution) contributes to the performance gap observed in synthetic training data.

To assess this effect, we use coverage and density metrics introduced by Naeem et al. [36] for synthetic data relative to real data. In short, density counts how many generated samples fall inside local neighborhoods around real images, while coverage measures the fraction of real images that have least one generated sample in their local neighborhood. These metrics provide complementary insights into how well the synthetic data distribution aligns with the real one. High density combined with low coverage indicates

over-concentration (*i.e.*, a collapsed or partially shifted synthetic manifold), while jointly low density and coverage imply a substantial domain shift. We calculate density and coverage metrics with respect to the real training dataset using CLIP-ViT-L’s vision head as a feature extractor. To obtain an accurate estimate of these metrics, we use 100 000 random samples.

We further probe the relationship between the data distribution and the Synth \rightarrow Real transfer performance (*i.e.*, training a classifier on synthetic data and evaluating it on real data) by comparing it with the performance obtained by testing a model fitted to real data on synthetic test data denoted as Real \rightarrow Synth. If there is a significant asymmetry towards the latter, it suggests that the synthetic dataset forms overly separable clusters that are easy for real-trained models to classify, yet fail to capture the complex decision boundaries present in real data.

4. Experiments

We evaluate thirteen open-source T2I models released between 2022 and 2025 to test whether generative progress translates into better synthetic training data. For every model, we measure Synth \rightarrow Real transfer performance and isolate the effects of prompt detail, texture fidelity, spectral (im-)balance, and distributional diversity.

4.1. Setup

The following paragraphs describe the data generation process, prompting schemes, and training configurations used throughout this paper.

Dataset Generators. We generate synthetic training datasets using a representative set of open-source T2I diffusion models released between 2022 and 2025. Our selection spans multiple generations of model design and scale, allowing us to trace how architectural and training advances affect downstream data utility. Specifically, we include Stable Diffusion V1.5 (2022) [43], Stable Diffusion 2.1 (2023) [43], Stable Diffusion XL (2023) [38], Stable Diffusion 3.5 (2024) [50] (large and medium), Sana (2024) [11], Flux-Dev (2024) [28], Qwen-Image (2025) [57], and Lumina 2.0 (2025) [39]. To evaluate efficiency-oriented variants, we also include distilled counterparts, *i.e.*, SDXL-Turbo (2023) [38], Stable Diffusion 3.5-Large-Turbo (2024) [11], and Flux-Schnell (2024) [28].

Datasets. Following prior work on synthetic image evaluation [12, 47, 49], we use image classification on ImageNet-1k as our benchmark task. To reduce computational cost during training, following the TinyImageNet protocol [29], we create a reduced training subset of ImageNet-1k by randomly

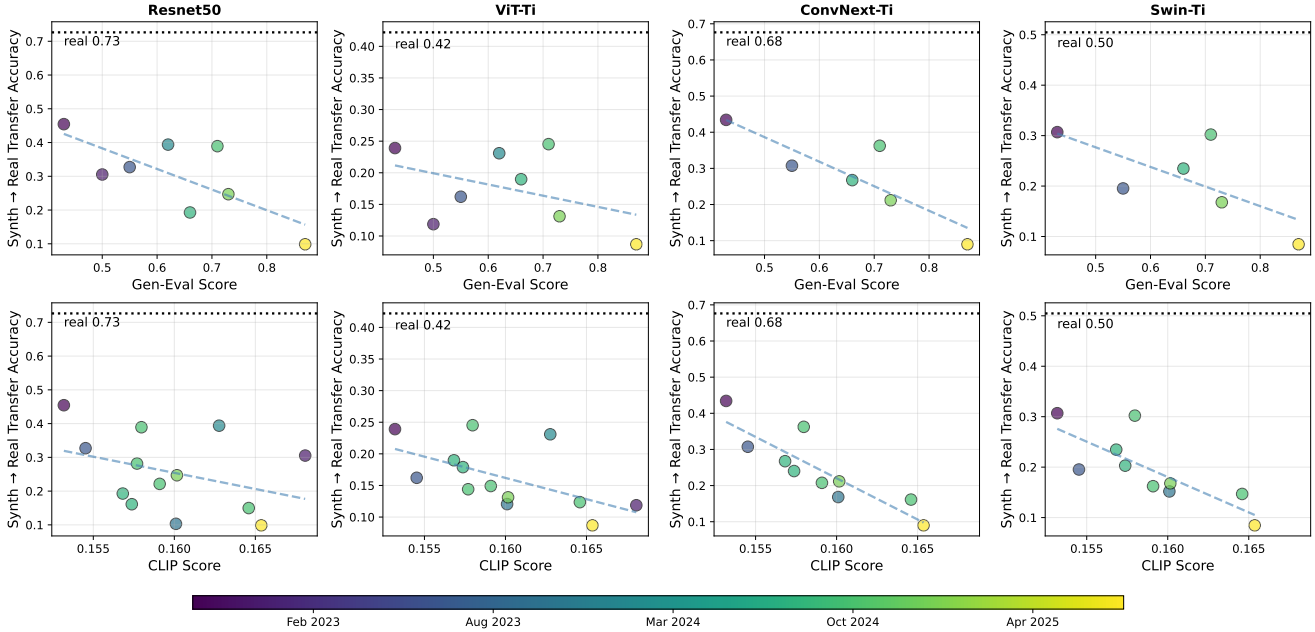


Figure 3. Accuracy on the real ImageNet-1k test set versus GenEval score (**top**) and CLIPScore (**bottom**). Each point represents the performance of a classifier trained on data synthesized by a specific T2I model; the horizontal line indicates the baseline trained on real data. Across architectures, we observe a downward trend; higher benchmark scores correspond to lower transfer performance for class label prompts.

sampling 200 classes and 500 images per class (100 000 images in total). For testing, we use images from the validation set corresponding to the sampled classes without any additional sampling (IPC=50).

T2I Generation. We use a low classifier-free guidance scale of 2.0 and 50 denoising steps to balance fidelity and diversity [21, 47]. For distilled “turbo” models, we use four denoising steps. All models except SDXL, which requires generation at 1024×1024 pixels, produce 512×512 pixel images. All images are then down-sampled to 256×256 .

Prompts. We use two types of prompts for T2I generation to determine the impact of text inputs: (i) class names and (ii) detailed captions. Detailed captions are produced by recaptioning real images from our training set using GPT-4.1-nano. We prompt the LLM to produce a two to three-sentence description for each image that captures the background, foreground, and describes all visible objects. Prompts from detailed captions follow the template by Singh et al. [49] (“*[class name], [caption]*”) to ensure alignment with the label, even if the prompt fails to mention the class name.

Detailed captions obtained by recaptioning real data serve as a best-case scenario for T2I generation. However, it is worth noting that this scenario is impractical, as original images are usually *not* available in the fully synthetic T2I

dataset generation case. Additionally, recaptioning each image requires substantial computational cost for large datasets.

Classification Models. Our primary architecture is ResNet-50 [22]. To test the generality of observed trends, we additionally evaluate ViT-Ti [10], ConvNeXt-Ti [32], and Swin-Ti [31] on RGB data. All models are trained for 80 epochs with a batch size of 1024 using the Adam optimizer with a learning rate of 10^{-3} , five epochs of linear warm-up, and a cosine-annealing learning rate schedule. Models are validated each epoch on validation data from the training domain (models trained on synthetic data are validated on synthetic data), and the checkpoint with the lowest validation loss is used for evaluation on real data.

4.2. Performance Gap Trends

We begin by examining whether progress in T2I model development translates to better performance when synthetic images are used as training data.

Figure 1 visualizes the performance of models trained class name-conditioned synthetic data on the real test set over time, while Figure 3 relates it to the performance on standard T2I alignment metrics. We consider GenEval [18], which measures how well text-specified fine-grained object properties (color, position, object count) are represented in the output image, and ClipScore [23], which measures general alignment between prompt and images

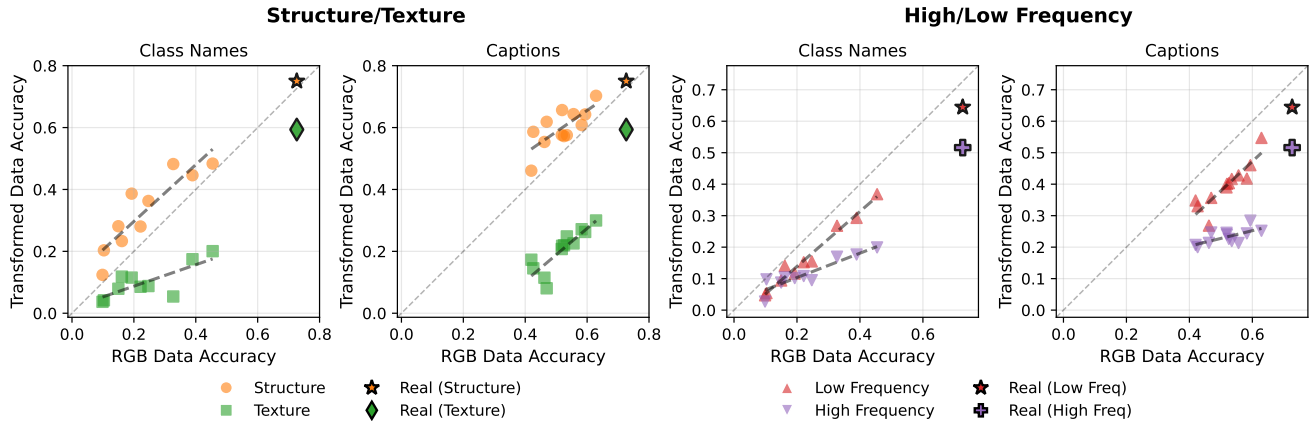


Figure 4. Performance comparison for (left) structure (depth-based classifier) and texture (local feature classifier), and (right) frequency-filtered data for class name- and caption-guided synthetic datasets. Image structure is consistently less affected than texture, while high-frequency components degrade more strongly than low frequencies (especially in better-performing models).

in CLIP’s shared language-vision embedding space. We report GenEval scores as computed by Wu et al. [57] and calculate CLIP-ViT-L scores using image-text pairs from the detailed captions condition.

Benchmark results align with intuition and conclusions reported by respective models. Newer models score higher on text-alignment metrics as the field progresses. This is not unexpected, as achieving controllable T2I synthesis is a major goal in the field of image generation. However, we also find a surprising trend: Text-to-image alignment is *inversely* related to synthetic data performance in the class name-conditioned scenario. These results suggest a hidden tradeoff between prompt following and the performance of a given model as a training data generator.

4.3. Texture and Structure

Figure 4 (left) plots ResNet-50 RGB space performance against the performance of classifiers operating in texture and structure spaces. First, we observe that, for both class names and caption prompts and across all tested models, there is a significant difference between the performance gaps observed in texture and structure space. Classifiers operating in the structure space consistently demonstrate a much narrower gap to real data than is the case for texture space classifiers.

Models with higher RGB accuracy also display a higher accuracy in *both* texture and structure space, suggesting that *both* image structure and texture affect accuracy on RGB data. Additionally, we observe that the removal of textural information reduces the Synth. \rightarrow Real gap, compared to the Synth. \rightarrow Real gap in RGB space (*i.e.*, structure space models are above the diagonal in Figure 4 (left)), suggesting that synthetic textures hinder the transferability of models from synthetic to real data.

Although using detailed captions improves performance in both RGB and structure spaces, the improvement in the texture space is only minimal. This suggests that the presence of low-level artifacts affecting textures is largely decoupled from input captions and, unlike the image structure, cannot be significantly alleviated by better captions.

In practical terms, modern T2I models demonstrate good prompt following and produce images that can appear coherent and realistic to human observers but lack the textural diversity that neural networks rely on for generalization. Thus, improvements in global composition and realism may conceal a growing deficit in textural richness, limiting the effectiveness of synthetic data for training vision models.

4.4. Power Spectrum

Figure 4 (right) showcases ResNet-50 RGB space performance against the performance of classifiers operating on high and low frequency images. The obtained results mirror those from the texture/structure experiment. Performance in the low-frequency domain closely follows the RGB domain, suggesting that smooth spatial transitions and global contrast are faithfully preserved by synthetic images. This is in contrast to the high-frequency domain, where a more significant gap to RGB space is observed. Additionally, as in the texture/structure domain experiment, providing detailed captions does not significantly improve high-frequency domain performance; especially compared to improvements in the low-frequency domain.

Together with the texture-structure results, these findings indicate that modern T2I models have become increasingly structure-accurate but texture-deficient. Low-frequency details are generally accurate and can be improved with better text input, while high-frequency details remain broken.

4.5. Distribution and Diversity

Figure 5 summarizes the relationship between density, coverage, and transfer accuracy. We find that as density decreases and coverage increases, the transfer accuracy to real data increases. Many poorly performing models exhibit high density, suggesting their distributions are collapsed. However, some models, such as SDXL, Sana, or SD2.1, exhibit low density with low coverage, suggesting a significant shift in image distributions. Using detailed captions derived from real data significantly increases coverage and reduces density. This change is especially pronounced for models that perform poorly when using class names as prompts.

To further probe this relationship, Figure 6 compares cross-domain transfer: How well does a model trained on real data classify synthetic images (Real \rightarrow Synth.) compared to the reverse (Synth. \rightarrow Real)? For class name prompts, generated data results in poor Synth. \rightarrow Real accuracy; however, Real \rightarrow Synth transfer is comparatively high. Using detailed captions improves Synth. \rightarrow Real transfer and partially reduces this asymmetry.

Results from this experiment extend observations from density and coverage measurements shown in Figure 5. Together, these two results imply that existing T2I models tend to prioritize *sample realism* over *distributional realism*. Individual synthetic images tend to remain relatively easy to classify for a model trained on real data, suggesting that *sample realism* remains relatively intact. However, *distributional realism* is significantly degraded as suggested by density and coverage values, leading to poor model transfer to real data. For the class name prompts, the collapsed distribution indicated by high density values appears to be the dominant factor driving the gap, while for detailed captions, the distribution shift indicated by lower coverage appears to be the dominant factor.

The significant difference in density and coverage between the class name and detailed prompts suggests that high prompt-following comes at the cost of a distribution collapse and/or shift, making recent T2I models unsuitable for synthetic data generation unless highly detailed captions are first obtained.

5. Discussion

Our results identify multiple patterns that significantly affect the utility of modern T2I models as synthetic data generators.

Prompt Following - Performance Tradeoff. We find that these models exhibit a significant trade-off between prompt following and data distribution quality for simple prompts. Newer T2I models only increase performance when the prompts describe images in detail (Figure 5), while class name prompts lead to a significant performance regression in newer models (Figure 5, Figure 1). Prompt following

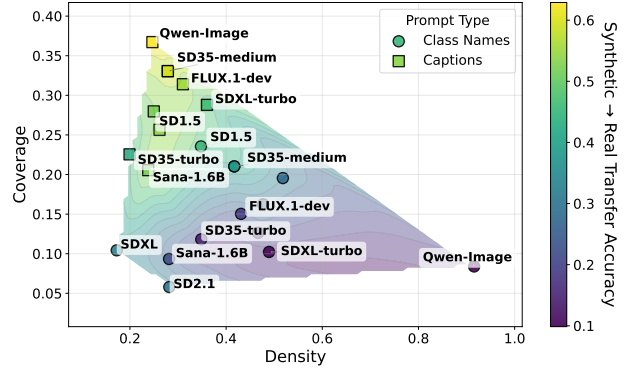


Figure 5. Dataset diversity using density and coverage metrics from Naeem et al. [36], plotted against classifier accuracy on real data (color). Models with high density but low coverage produce visually consistent yet distributionally narrow samples, while those with higher coverage span a broader portion of real data space and correlate with better generalization. Thus, recent T2I models achieve higher sample quality through compact, high-density clusters but sacrifice diversity essential for training quality.

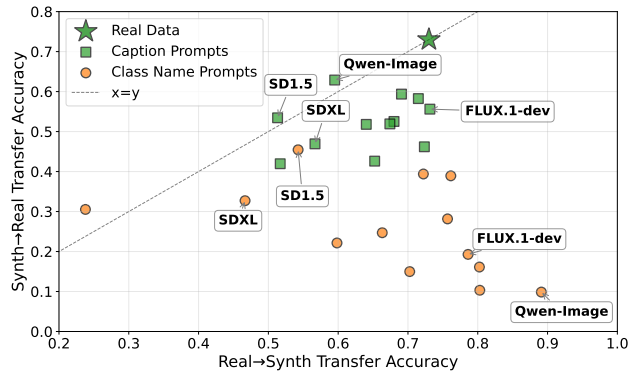


Figure 6. Comparison of cross-domain transfer for ResNet-50: classification accuracy of models trained on real data and evaluated on synthetic images (Real \rightarrow Synth) versus the reverse setting (Synth \rightarrow Real). Synthetic data are increasingly easy for real-trained models to classify, yet models trained on synthetic data transfer progressively worse to real test images, revealing growing asymmetry between visual and learning alignment.

scores increase while the classifier model transfer to real data decreases (Figure 3).

Persistent Lack of High Frequency Realism. We find that texture and high-frequency details in synthetic vision data are significantly more affected than structure and low-frequency details (Figure 4). If textures are removed from the image (via depth estimation), the performance gap is reduced compared to the RGB space. Respectively, the texture classifier exhibits a significantly higher gap to real data than networks operating in RGB and depth space. Those conclu-

sions are further supported by measurements of the performance gap on high- and low-frequency filtered images. The gap is higher in high-frequency space than in low-frequency space. Moreover, in the best-case scenario, using high-detail captions only significantly improves low-frequency details and the image’s structure. The performance gap in texture and high-frequency spaces remains high, suggesting that high-frequency realism is mostly decoupled from the text input.

Sample vs Data Realism. Most models show a strong mismatch between Real \rightarrow Synth. and Synth. \rightarrow Real transfer (Figure 6). Real-trained classifiers handle synthetic images well, but synthetic-trained classifiers generalize poorly to real data. Density-coverage analyses explain this asymmetry: class-label prompts produce high-density, low-coverage datasets that collapse around narrow aesthetic modes. Detailed captions improve both density and coverage, showing that low-detail prompts encourage sampling from an overly concentrated subset of the manifold. In short, synthetic samples look realistic enough to classify, but the overall dataset does not reflect real-world variation and decision boundaries.

6. Limitations & Future Work

Our experiments target image classification on a 200-class subset of ImageNet-1k, chosen to balance scale and computational feasibility. The observed trends may differ in other domains, such as detection or segmentation, or under larger training datasets. We also restrict our evaluation to publicly available T2I models. A broader study across proprietary or closed models could refine observed trends. However, the usefulness of proprietary models for large-scale training data synthesis is limited for a wider community due to restricted access to large-scale inference.

Future work on developing new T2I models should prioritize diversity rather than surface realism, encouraging generators to produce richer textures and more natural frequency statistics instead of optimizing primarily for aesthetic appeal. It is equally important to evaluate usefulness directly, *i.e.*, by incorporating learnability checks (such as density-coverage measurements), so that improvements in visual realism align more with data realism. Finally, future work may need to couple generation with learning more, allowing lightweight classifier signals to shape the generation toward improved learnability.

7. Conclusion

Modern T2I models generate data that looks aesthetically better but functions worse as reliable training data. Across fourteen generators and multiple classifiers, we find that progress in visual fidelity and improved prompt following does *not* lead to better synthetic training data. Our analysis

points to three drivers of this trend: First, high-frequency details are degraded, removing class-discriminative cues that image recognition models rely on. Second, there is a growing structure-texture imbalance: global composition and layout improve, while fine-scale variation collapses. Third, the data distribution narrows, leading to high density but low coverage in feature space. Detailed prompts can partially improve structure, but they do *not* fix the core texture and high-frequency domain issues.

We thus advocate for three practical shifts: First, train for diversity and natural image statistics, not only for photorealism. Second, report utility alongside perceptual quality by including density-coverage metrics, probing classification models by training on synthetic and testing on real data, and frequency-band transfer results. Third, design prompts and distillation pipelines that preserve intra-class variation and fine details. Closing this gap will require coupling generation with learning and rewarding diversity where it matters most: in the features that make models generalize.

References

- [1] Pietro Astolfi, Marlene Careil, Melissa Hall, Oscar Mañas, Matthew Muckley, Jakob Verbeek, Adriana Romero Soriano, and Michal Drozdal. Consistency-diversity-realism pareto fronts of conditional image generative models. *arXiv*, 2024. 3, 4
- [2] Manel Baradad Jurjo, Jonas Wulff, Tongzhou Wang, Phillip Isola, and Antonio Torralba. Learning to see by looking at noise. *NeurIPS*, 2021. 4
- [3] Antonella Barisic, Frano Petric, and Stjepan Bogdan. Sim2air-synthetic aerial dataset for uav monitoring. *IEEE Robotics and Automation Letters*, 2022. 1
- [4] Ali Borji. Pros and cons of gan evaluation measures: New developments. *Computer Vision and Image Understanding*, 2022. 4
- [5] Wieland Brendel and Matthias Bethge. Approximating cnns with bag-of-local-features models works surprisingly well on imagenet. *arXiv*, 2019. 4
- [6] George Cazenavette, Tongzhou Wang, Antonio Torralba, Alexei A Efros, and Jun-Yan Zhu. Generalizing dataset distillation via deep generative prior. In *CVPR*, 2023. 3
- [7] Dong Chen, Xinda Qi, Yu Zheng, Yuzhen Lu, Yanbo Huang, and Zhaojian Li. Deep data augmentation for weed recognition enhancement: A diffusion probabilistic model and transfer learning based approach. In *2023 ASABE Annual International Meeting*. American Society of Agricultural and Biological Engineers, 2023. 1
- [8] Zeming Chen, Alejandro Hernández Cano, Angelika Romanou, Antoine Bonnet, Kyle Matoba, Francesco Salvi, Matteo Pagliardini, Simin Fan, Andreas Köpf, Amirkeivan Mhtashami, et al. Meditron-70b: Scaling medical pretraining for large language models. *arXiv*, 2023. 1
- [9] Riccardo Corvi, Davide Cozzolino, Giovanni Poggi, Koki Nagano, and Luisa Verdoliva. Intriguing properties of synthetic images: from generative adversarial networks to diffusion models. In *CVPR*, 2023. 3, 4

- [10] Alexey Dosovitskiy. An image is worth 16x16 words: Transformers for image recognition at scale. *arXiv*, 2020. 5
- [11] Patrick Esser, Sumith Kulal, Andreas Blattmann, Rahim Entezari, Jonas Müller, Harry Saini, Yam Levi, Dominik Lorenz, Axel Sauer, Frederic Boesel, et al. Scaling rectified flow transformers for high-resolution image synthesis. 2024. 1, 4
- [12] Lijie Fan, Kaifeng Chen, Dilip Krishnan, Dina Katabi, Phillip Isola, and Yonglong Tian. Scaling laws of synthetic images for model training... for now. In *CVPR*, 2024. 2, 4
- [13] Haoyang Fang, Boran Han, Shuai Zhang, Su Zhou, Cuixiong Hu, and Wen-Ming Ye. Data augmentation for object detection via controllable diffusion models. In *CVPR*, 2024. 2
- [14] Stanislav Fort and Jonathan Whitaker. Direct ascent synthesis: Revealing hidden generative capabilities in discriminative models. *arXiv*, 2025. 4
- [15] Paul Gavrikov and Janis Keuper. Can biases in imagenet models explain generalization? In *CVPR*, 2024. 4
- [16] Robert Geirhos, Patricia Rubisch, Claudio Michaelis, Matthias Bethge, Felix A Wichmann, and Wieland Brendel. Imagenet-trained cnns are biased towards texture; increasing shape bias improves accuracy and robustness. In *ICLR*, 2018. 3
- [17] Scott Geng, Cheng-Yu Hsieh, Vivek Ramanujan, Matthew Wallingford, Chun-Liang Li, Pang Wei W Koh, and Ranjay Krishna. The unmet promise of synthetic training images: Using retrieved real images performs better. *NeurIPS*, 2024. 2, 3
- [18] Dhruva Ghosh, Hannaneh Hajishirzi, and Ludwig Schmidt. Geneval: An object-focused framework for evaluating text-to-image alignment. *NeurIPS*, 2023. 5
- [19] Aldren Gonzales, Guruprabha Guruswamy, and Scott R Smith. Synthetic data in health care: A narrative review. *PLOS Digital Health*, 2023. 1, 2
- [20] Aaron Grattafiori, Abhimanyu Dubey, Abhinav Jauhri, Abhinav Pandey, Abhishek Kadian, Ahmad Al-Dahle, Aiesha Letman, Akhil Mathur, Alan Schelten, Alex Vaughan, et al. The llama 3 herd of models. *arXiv*, 2024. 1
- [21] Hasan Abed Al Kader Hammoud, Hani Itani, Fabio Pizzati, Philip Torr, Adel Bibi, and Bernard Ghanem. Synthclip: Are we ready for a fully synthetic clip training? *arXiv*, 2024. 2, 5
- [22] Kaiming He, Xiangyu Zhang, Shaoqing Ren, and Jian Sun. Deep residual learning for image recognition. In *CVPR*, 2016. 5
- [23] Jack Hessel, Ari Holtzman, Maxwell Forbes, Ronan Le Bras, and Yejin Choi. Clipscore: A reference-free evaluation metric for image captioning. In *Proceedings of the 2021 conference on empirical methods in natural language processing*, 2021. 5
- [24] Joel Hestness, Sharan Narang, Newsha Ardalani, Gregory Diamos, Heewoo Jun, Hassan Kianinejad, Md Mostofa Ali Patwary, Yang Yang, and Yanqi Zhou. Deep learning scaling is predictable, empirically. *arXiv*, 2017. 1
- [25] Jared Kaplan, Sam McCandlish, Tom Henighan, Tom B Brown, Benjamin Chess, Rewon Child, Scott Gray, Alec Radford, Jeffrey Wu, and Dario Amodei. Scaling laws for neural language models. *arXiv*, 2020. 1
- [26] Junsu Kim, Hoseong Cho, Jiheon Kim, Yihalem Yimolal Tiruneh, and Seungryul Baek. Sddgr: Stable diffusion-based deep generative replay for class incremental object detection. In *CVPR*, 2024. 2
- [27] Lennart R Koetzier, Jie Wu, Domenico Mastrodicasa, Aline Lutz, Matthew Chung, W Adam Koszek, Jayanth Pratap, Akshay S Chaudhari, Pranav Rajpurkar, Matthew P Lungren, et al. Generating synthetic data for medical imaging. *Radiology*, 2024. 1, 2
- [28] Black Forest Labs. Flux.1 [dev] – 12 b-parameter text-to-image model. <https://huggingface.co/black-forest-labs/FLUX.1-dev>, 2024. 1, 2, 4
- [29] Yann Le and Xuan Yang. Tiny imagenet visual recognition challenge. *CS 231N*, 2015. 4
- [30] Shiye Lei, Hao Chen, Sen Zhang, Bo Zhao, and Dacheng Tao. Image captions are natural prompts for text-to-image models. *arXiv*, 2023. 2
- [31] Ze Liu, Yutong Lin, Yue Cao, Han Hu, Yixuan Wei, Zheng Zhang, Stephen Lin, and Baining Guo. Swin transformer: Hierarchical vision transformer using shifted windows. In *CVPR*, 2021. 5
- [32] Zhuang Liu, Hanzi Mao, Chao-Yuan Wu, Christoph Feichtenhofer, Trevor Darrell, and Saining Xie. A convnet for the 2020s. In *CVPR*, 2022. 5
- [33] Eugenio Lomurno, Matteo D’Oria, and Matteo Matteucci. Stable diffusion dataset generation for downstream classification tasks. *arXiv*, 2024. 2
- [34] Sergi Masip, Pau Rodriguez, Tinne Tuytelaars, and Gido M van de Ven. Continual learning of diffusion models with generative distillation. *arXiv*, 2023. 2
- [35] Brian B Moser, Federico Raue, Sebastian Palacio, Stanislav Frolov, and Andreas Dengel. Latent dataset distillation with diffusion models. *arXiv*, 2024. 3
- [36] Muhammad Ferjad Naeem, Seong Joon Oh, Youngjung Uh, Yunjey Choi, and Jaejun Yoo. Reliable fidelity and diversity metrics for generative models. 2020. 4, 7
- [37] Maxime Oquab, Timothée Darcet, Theo Moutakanni, Huy V. Vo, Marc Szafraniec, Vasil Khalidov, Pierre Fernandez, Daniel Haziza, Francisco Massa, Alaaeldin El-Nouby, Russell Howes, Po-Yao Huang, Hu Xu, Vasu Sharma, Shang-Wen Li, Wojciech Galuba, Mike Rabbat, Mido Assran, Nicolas Ballas, Gabriel Synnaeve, Ishan Misra, Herve Jegou, Julien Mairal, Patrick Labatut, Armand Joulin, and Piotr Bojanowski. DINOv2: Learning robust visual features without supervision, 2023. 1
- [38] Dustin Podell, Zion English, Kyle Lacey, Andreas Blattmann, Tim Dockhorn, Jonas Müller, Joe Penna, and Robin Rombach. Sdxl: Improving latent diffusion models for high-resolution image synthesis. *arXiv*, 2023. 1, 2, 4
- [39] Qi Qin, Le Zhuo, Yi Xin, Ruoyi Du, Zhen Li, Bin Fu, Yiting Lu, Jiakang Yuan, Xinyue Li, Dongyang Liu, et al. Lumina-image 2.0: A unified and efficient image generative framework. *arXiv*, 2025. 2, 4
- [40] Vivek Ramanujan, Thao Nguyen, Sewoong Oh, Ali Farhadi, and Ludwig Schmidt. On the connection between pre-training data diversity and fine-tuning robustness. *NeurIPS*, 2023. 1

- [41] Aditya Ramesh, Prafulla Dhariwal, Alex Nichol, Casey Chu, and Mark Chen. Hierarchical text-conditional image generation with clip latents. *arXiv*, 2022. 2
- [42] Nikhila Ravi, Valentin Gabeur, Yuan-Ting Hu, Ronghang Hu, Chaitanya Ryali, Tengyu Ma, Haitham Khedr, Roman Rädle, Chloe Rolland, Laura Gustafson, Eric Mintun, Junting Pan, Kalyan Vasudev Alwala, Nicolas Carion, Chao-Yuan Wu, Ross Girshick, Piotr Dollár, and Christoph Feichtenhofer. Sam 2: Segment anything in images and videos. *arXiv*, 2024. 1
- [43] Robin Rombach, Andreas Blattmann, Dominik Lorenz, Patrick Esser, and Björn Ommer. High-resolution image synthesis with latent diffusion models. In *CVPR*, 2022. 1, 2, 4
- [44] Thomas Rothmeier, Werner Huber, and Alois C Knoll. Time to shine: Fine-tuning object detection models with synthetic adverse weather images. In *CVPR*, 2024. 2
- [45] Chitwan Saharia, William Chan, Saurabh Saxena, Lala Li, Jay Whang, Emily L Denton, Kamyar Ghasemipour, Raphael Gontijo Lopes, Burcu Karagol Ayan, Tim Salimans, et al. Photorealistic text-to-image diffusion models with deep language understanding. *NeurIPS*, 2022. 2, 4
- [46] Fatemeh Saleh, Sadegh Aliakbarian, Charlie Hewitt, Lohit Petikam, Xian Xiao, Antonio Criminisi, Thomas J Cashman, and Tadas Baltrusaitis. David: Data-efficient and accurate vision models from synthetic data. In *CVPR*, 2025. 2
- [47] Mert Bülent Saryıldız, Karteek Alahari, Diane Larlus, and Yannis Kalantidis. Fake it till you make it: Learning transferable representations from synthetic imagenet clones. In *CVPR*, 2023. 2, 4, 5
- [48] Minhyuk Seo, Seongwon Cho, Minjae Lee, Diganta Misra, Hyeonbeom Choi, Seon Joo Kim, and Jonghyun Choi. Just say the name: Online continual learning with category names only via data generation. *arXiv*, 2024. 2
- [49] Krishnakant Singh, Thanush Navaratnam, Jannik Holmer, Simone Schaub-Meyer, and Stefan Roth. Is synthetic data all we need? benchmarking the robustness of models trained with synthetic images. In *CVPR*, 2024. 2, 4, 5
- [50] Stability AI. Introducing stable diffusion 3.5. <https://stability.ai/news/introducing-stable-diffusion-3-5>, 2024. Accessed: 2025-11-12. 4
- [51] Duo Su, Junjie Hou, Weizhi Gao, Yingjie Tian, and Bowen Tang. D⁴m: Dataset distillation via disentangled diffusion model. In *CVPR*, 2024. 3
- [52] Yonglong Tian, Lijie Fan, Phillip Isola, Huiwen Chang, and Dilip Krishnan. Stablerep: Synthetic images from text-to-image models make strong visual representation learners. *NeurIPS*, 2023. 2
- [53] Yonglong Tian, Lijie Fan, Kaifeng Chen, Dina Katabi, Dilip Krishnan, and Phillip Isola. Learning vision from models rivals learning vision from data. In *CVPR*, 2024. 2
- [54] Vishaal Udandarao, Ameya Prabhu, Adhiraj Ghosh, Yash Sharma, Philip Torr, Adel Bibi, Samuel Albanie, and Matthias Bethge. No” zero-shot” without exponential data: Pretraining concept frequency determines multimodal model performance. *NeurIPS*, 2024. 1
- [55] Roy Voetman, Maya Aghaei, and Klaas Dijkstra. The big data myth: Using diffusion models for dataset generation to train deep detection models. *arXiv*, 2023. 2
- [56] Jiaxiao Wen, Tao Chu, and Qiong Liu. Highly realistic synthetic dataset for pixel-level densepose estimation via diffusion model. *Pattern Recognition*, 2025. 2
- [57] Chenfei Wu, Jiahao Li, Jingren Zhou, Junyang Lin, Kaiyuan Gao, Kun Yan, Sheng-ming Yin, Shuai Bai, Xiao Xu, Yilei Chen, et al. Qwen-image technical report. *arXiv*, 2025. 1, 2, 4, 6
- [58] Jia Xu, Cheng Yuan, Jiakuan Gu, Jian Liu, Jiong An, and Qingzhao Kong. Innovative synthetic data augmentation for dam crack detection, segmentation, and quantification. *Structural Health Monitoring*, 2023. 1
- [59] Jiahao Yang, Wufei Ma, Angtian Wang, Xiaoding Yuan, Alan Yuille, and Adam Kortylewski. Robust category-level 3d pose estimation from diffusion-enhanced synthetic data. In *CVPR*, 2024. 2
- [60] Lihe Yang, Bingyi Kang, Zilong Huang, Zhen Zhao, Xiaogang Xu, Jiashi Feng, and Hengshuang Zhao. Depth anything v2. *NeurIPS*, 2024. 3
- [61] Yongchao Zhou, Hshmat Sahak, and Jimmy Ba. Training on thin air: Improve image classification with generated data. *arXiv*, 2023. 2
- [62] Jingyuan Zhu, Shiyu Li, Yuxuan Andy Liu, Jian Yuan, Ping Huang, Jiulong Shan, and Huimin Ma. Odgen: Domain-specific object detection data generation with diffusion models. *NeurIPS*, 2024. 2

Appendix

A. Impact of the VAE

VAE	Acc_{pixel}	$Acc_{highpass}$	$Acc_{lowpass}$
-	73.0	51.6	64.5
SD1.5	70.5	37.6	63.1
SDXL	69.7	37.1	62.8
Flux	70.6	37.7	63.4

Table 1. We quantify the impact of the VAE by performing the reconstruction of our ImageNet subset and then training on it. An evaluation on unaltered real data reveals that the VAE accounts for a significant drop in accuracy in the high-frequency regime.

B. Additional Vision Tasks

In addition to classification, we test object detection and segmentation to determine whether the observed trend holds across other vision tasks. Tested models do not all support additional spatial ques, so we label generated images using the SAM3 model to obtain bounding boxes and segmentation masks. Due to computational constraints, we reuse the pixel-space images from the class-name case of the main experiment. To provide a fair comparison with real data, the same labelling method is applied to the ImageNet images.

For object detection, we follow torchvision¹ recipe and train object detection Faster-RCNN with Imagenet1k Resnet-50 backbone for 26 epochs with Adam optimizer and batch size of 16. For segmentation, we also follow the torchvision recipe for the DeepLabv3 model with Imagenet1k Resnet-50 backbone. We train the model using the Adam optimizer for 30 epochs with a batch size of 20.

B.1. Object Detection

Data Source	Test Scores		
	AP	AP ₅₀	AP ₇₅
ImageNet	20.2	47.6	14.1
SD V1.5 (Oct 2022)	11.9	32.1	6.2
SD V3.0 (Feb 2024)	11.0	28.7	6.4
Flux-dev (Aug 2024)	6.5	17.2	3.2
Lumina2 (Jan 2025)	6.1	17.3	3.2
Qwen-Image (Aug 2025)	3.1	8.2	1.7

Table 2. Performance of the Faster-RCNN model evaluated on the ImageNet validation subset labeled with SAM3 using the COCO evaluation protocol. We observe that the downward trend also applies to the object detection task, with the SD15 model outperforming recent state-of-the-art models.

B.2. Semantic Segmentation

Data Source	Test scores			
	Pixel Acc	mIoU	FWIoU	Dice Score
ImageNet	94.3	75.2	89.6	84.6
SD V1.5 (Oct 2022)	87.9	49.3	79.1	62.6
SD V3.0 (Feb 2024)	85.2	40.2	75.0	54.1
Flux-dev (Aug 2024)	78.2	27.9	66.5	40.6
Lumina2 (Jan 2025)	80.9	26.0	67.6	38.2
Qwen-Image (Aug 2025)	75.7	12.6	59.1	19.8

Table 3. Performance of the DeepLabv3 model evaluated on the ImageNet validation subset labeled with SAM3. We observe that the downward trend also applies to the semantic segmentation task, with the SD15 model outperforming recent state-of-the-art models.

C. Performance on Synthetic Test Set

Data Source	Real Test Set			Synth Test Set		
	Acc	AP	mIoU	Acc	AP	mIoU
Imagenet	73.0	20.2	47.6	-	-	-
SD1.5	45.5	11.9	49.3	79.6	25.5	71.2
SD2.1	30.5	-	-	51.6	-	-
SDXL	30.5	32.7	-	83.2	-	-
SDXL turbo	10.3	-	-	99.2	-	-
SD3.0	39.4	11.0	40.2	92.6	47.7	81.9
SD3.5 medium	38.9	-	-	94.6	-	-
SD3.5 large	28.2	-	-	77.6	-	-
SD3.5 turbo	15.0	-	-	97.6	-	-
Sana	22.1	-	-	97.3	-	-
Flux-dev	19.3	6.5	27.9	95.5	50.1	88.1
Flux-schnell	16.1	-	-	94.4	-	-
Lumina2	24.7	6.1	26.0	93.3	41.9	81.6
Qwen	9.9	3.1	12.6	97.9	69.5	93.7

Table 4. We evaluate the trained model on the same-sized synthetic validation set obtained from the same data source. We find that synthetic models generally achieve a much higher performance than on the real test set. This excludes bad fit as the source of the observed trend and instead strongly hints at a more easily class-separable data manifold. Accuracy (Acc) reported for the Resnet-50 network.

¹<https://github.com/pytorch/vision/tree/6f131f1f56f1b78c6301eb4>

D. Scaling Behavior of Synthetic Data

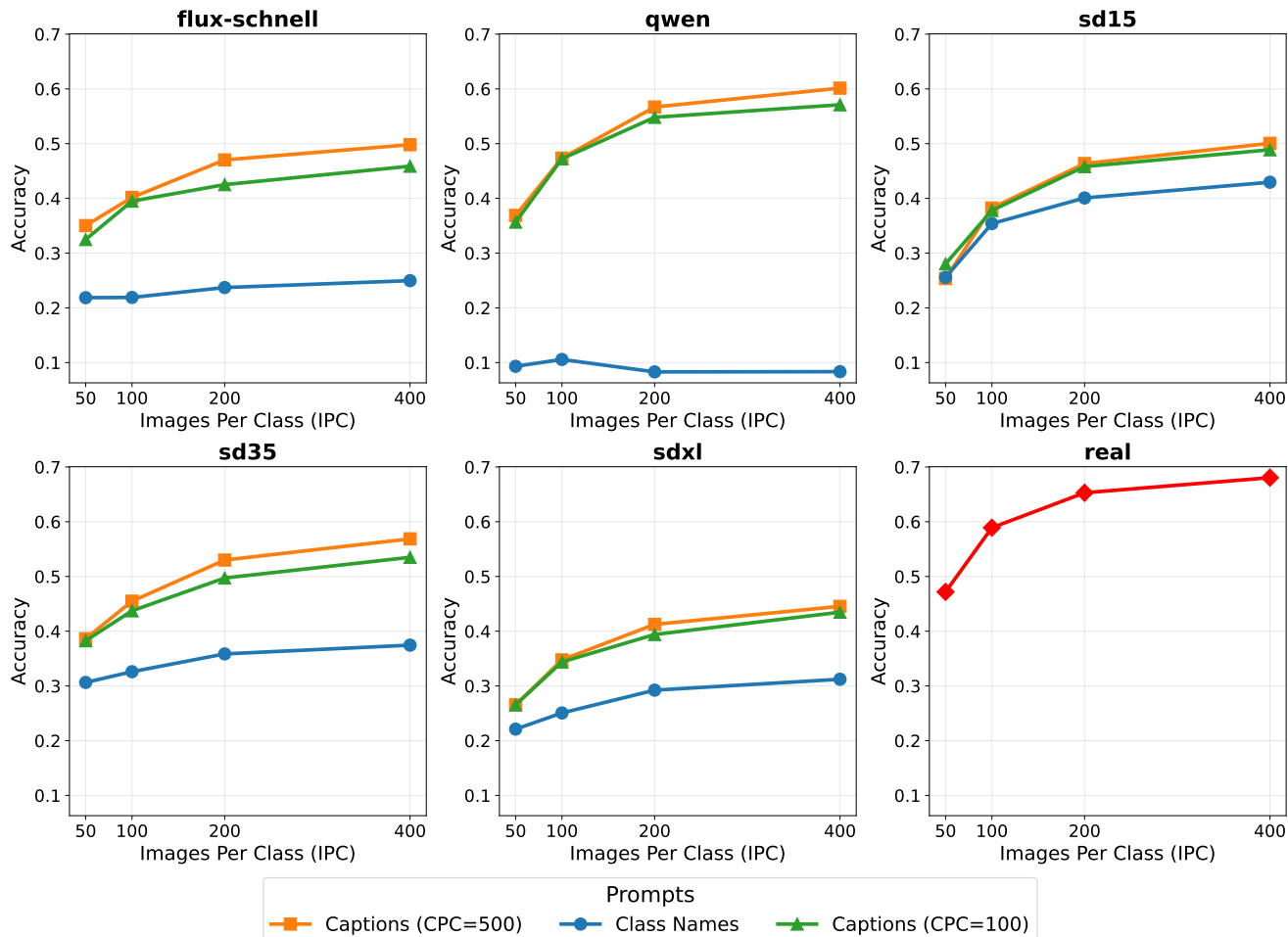


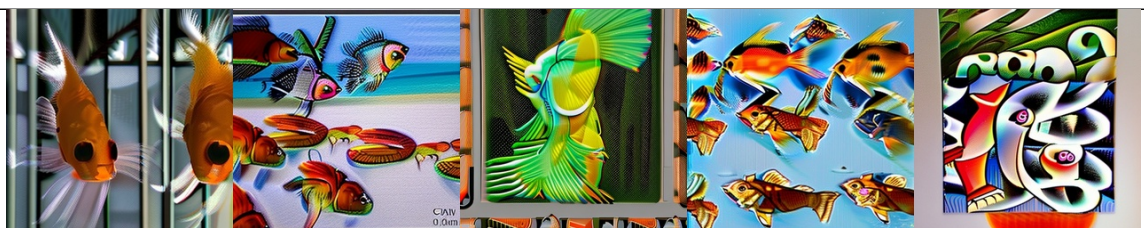

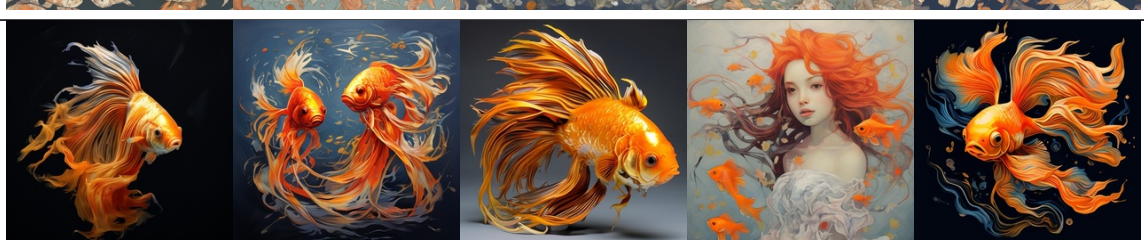


Figure 7. We investigate the scaling of the performance as a function of the number of Images per Class (IPC). We compare class-name prompts to image captions. We additionally test whether generating multiple images from the same caption impacts scaling. To test this, we also add a case in which the number of captions per class (CPC) is reduced to 100 (we generate 5 images per prompt). We observe that models which perform well with captions (qwen, flux-schnell, sd35). Exhibit a significant disparity between the scaling law of class name prompts and caption prompts. Additionally, we observe that when the number of unique prompts is reduced, those models also exhibit a bigger gap in scaling than models performing well with class names. This highlights the importance of using a diverse set of detail prompts for generation with recent models.

E. Synthetic Image Samples

Table 5. We visualize random samples from selected classes in the synthetic training dataset. Models are sorted by release date. Many of the tested models exhibit a distinct "visual style" that differs from real data. For example, select models (SDXL and pixelart) are biased towards stylistic, art-like images by default, rather than photorealistic images when the prompt is underspecified. Newer models tend to produce high-fidelity images; however, backgrounds often become blurry or plain, with the main object clearly visible and centered in the frame.

Data Source	Sample Images (Class Name Prompts)				
Goldfish					
ImageNet					
sd15					
sd21					
sdxl					
pixelart					

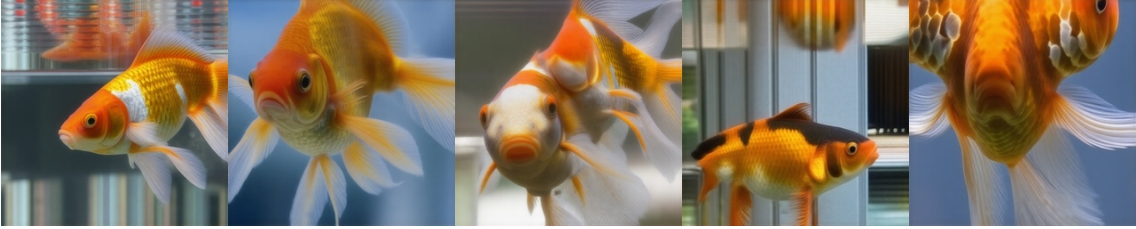

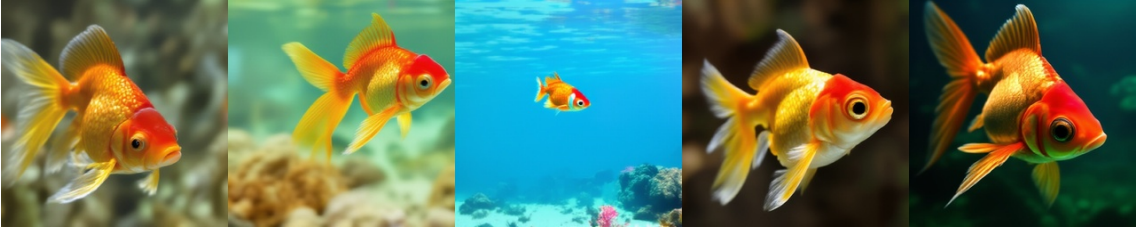



Continued on next page

Table 5 – Continued from previous page

Data Source	Sample Images (Class Name Prompts)				
sdxl-turbo					
sd30					
flux-dev					
flux-schnell					
sd35					
sd35-large					

Continued on next page

Table 5 – Continued from previous page

Data Source	Sample Images (Class Name Prompts)				
sd35-turbo					
sana					
lumina2					
qwen					
Monarch					
ImageNet					
sd15					


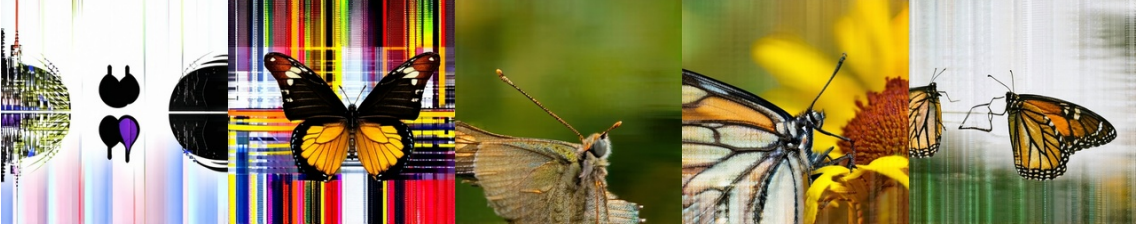

Continued on next page

Table 5 – Continued from previous page

Data Source	Sample Images (Class Name Prompts)				
sd21					
sdxl					
pixelart					
sdxl-turbo					
sd30					
flux-dev					







Continued on next page

Table 5 – Continued from previous page

Data Source	Sample Images (Class Name Prompts)
flux-schnell	
sd35	
sd35-large	
sd35-turbo	
sana	
lumina2	


Continued on next page

Table 5 – Continued from previous page

Data Source	Sample Images (Class Name Prompts)				
qwen					
Koala					
ImageNet					
sd15					
sd21					
sdxl					
pixelart					

Continued on next page

Table 5 – Continued from previous page

Data Source	Sample Images (Class Name Prompts)
sdxl-turbo	
sd30	
flux-dev	
flux-schnell	
sd35	
sd35-large	

Continued on next page

Table 5 – Continued from previous page

Data Source	Sample Images (Class Name Prompts)				
sd35-turbo					
sana					
lumina2					
qwen					
Broom					
ImageNet					
sd15					

Continued on next page

Table 5 – Continued from previous page

Data Source	Sample Images (Class Name Prompts)				
sd21					
sdxl					
pixelart					
sdxl-turbo					
sd30					
flux-dev					

Continued on next page

Table 5 – Continued from previous page









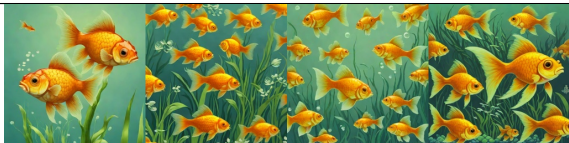
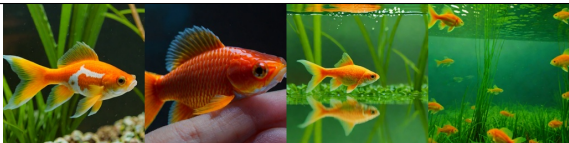

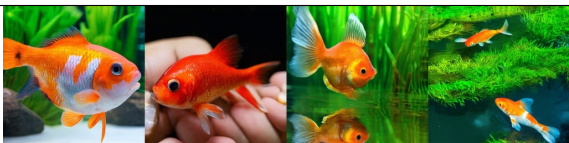
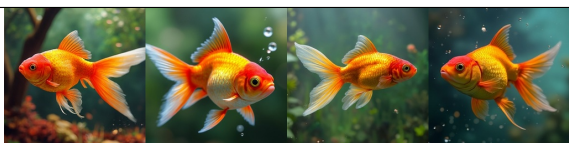
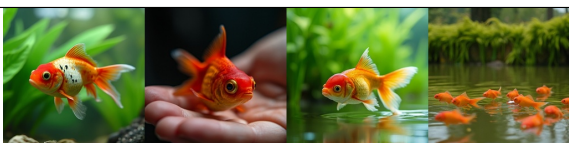
Data Source	Sample Images (Class Name Prompts)				
flux-schnell					
sd35					
sd35-large					
sd35-turbo					
sana					
lumina2					

Continued on next page

Table 5 – Continued from previous page





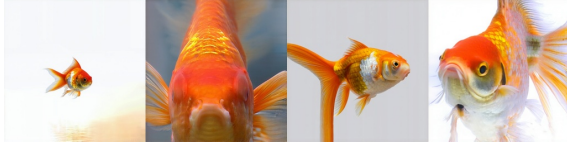
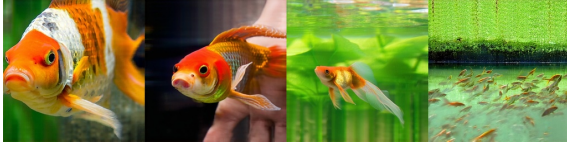
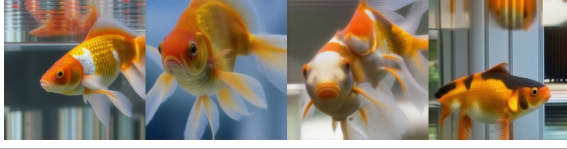
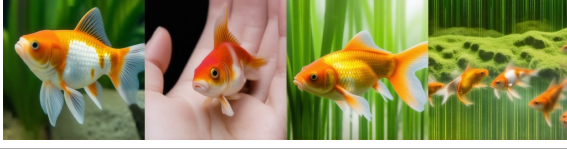
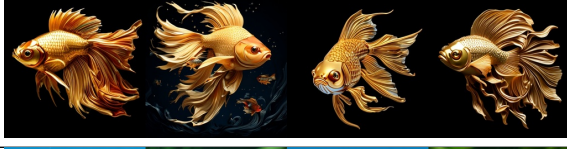
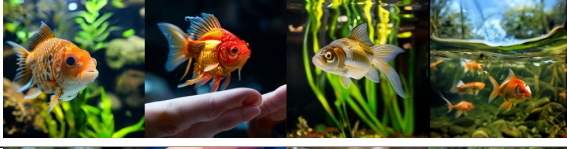

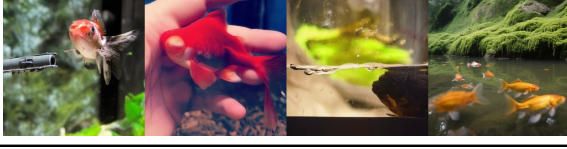
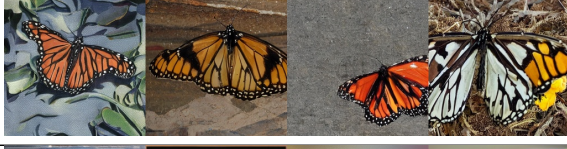


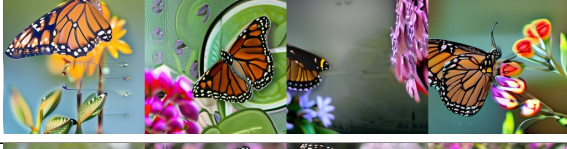
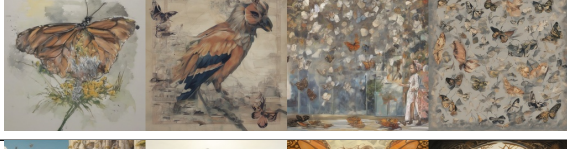
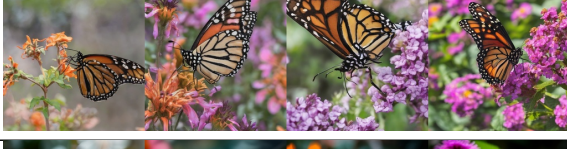
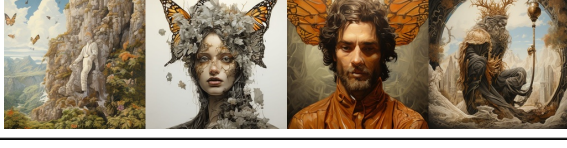

Data Source	Sample Images (Class Name Prompts)				
qwen					

Table 6. We visualize samples generated from images with class name and caption prompts. We see that using detailed captions significantly improves the diversity and realism of the synthetic data, matching the observed boost in model performance.

Model	Class Name Prompt	Caption Prompt
goldfish		
sd15		
sd21		
sdxl		
pixelart		
sdxl-turbo		
sd30		
flux dev		








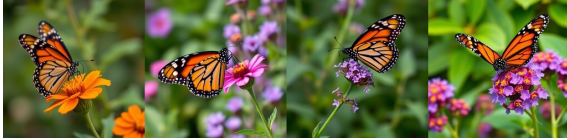




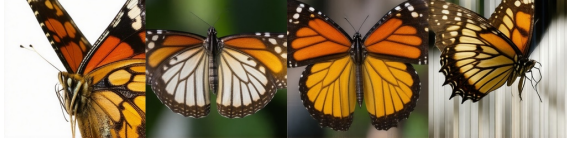
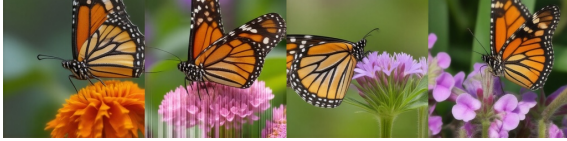






Continued on next page

Table 6 – Continued from previous page

Model	Class Name Prompt	Caption Prompt
flux-schnell		
sd35		
sd35-large		
sd35-turbo		
sana		
qwen		
monarch		
sd15		
sd21		
sdxl		
pixelart		








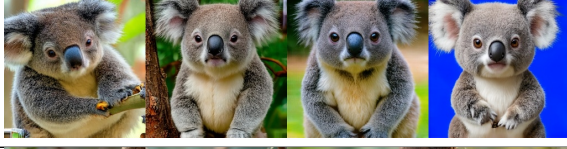



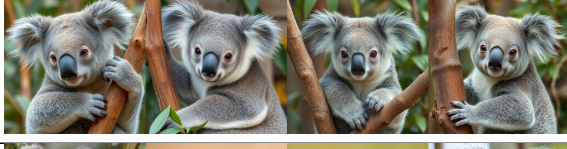


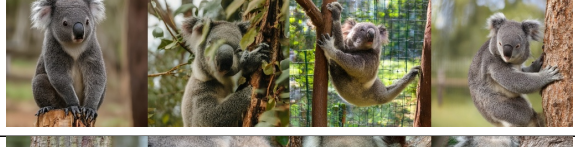
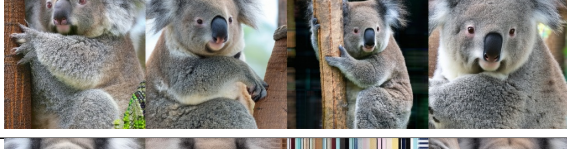
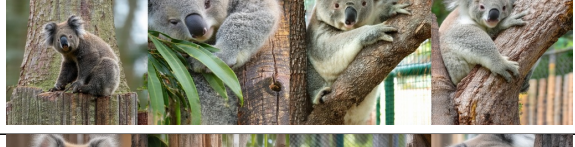
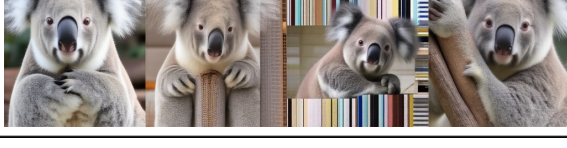

Continued on next page

Table 6 – Continued from previous page

Model	Class Name Prompt	Caption Prompt
sdxl-turbo		
sd30		
flux dev		
flux-schnell		
sd35		
sd35-large		
sd35-turbo		
sana		
qwen		
koala		
sd15		







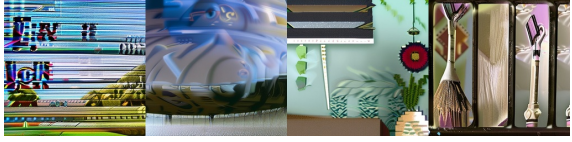



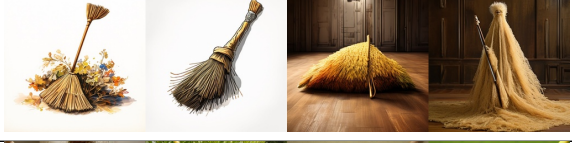



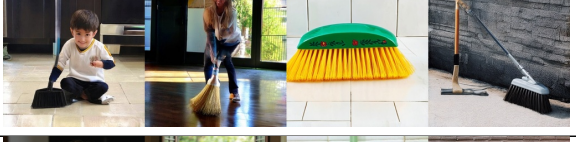




Continued on next page

Table 6 – Continued from previous page

Model	Class Name Prompt	Caption Prompt
sd21		
sdxl		
pixelart		
sdxl-turbo		
sd30		
flux dev		
flux-schnell		
sd35		
sd35-large		
sd35-turbo		

Continued on next page

Table 6 – Continued from previous page

Model	Class Name Prompt	Caption Prompt
sana		
qwen		
broom		
sd15		
sd21		
sdxl		
pixelart		
sdxl-turbo		
sd30		
flux dev		
flux-schnell		






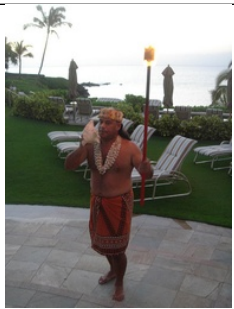
Continued on next page

Table 6 – Continued from previous page

Model	Class Name Prompt	Caption Prompt
sd35		
sd35-large		
sd35-turbo		
sana		
qwen		





F. Image Caption Samples

Table 7. The table below contains sample captions that were used as prompts in the paper. Captions were obtained through prompting the GPT4-nano model.

Image	Caption
	<p>The image features a woman standing on a wooden patio, framed by an open door in the foreground. She is holding a large umbrella against the backdrop of a brick house and a small garden area, with outdoor furniture and a grayish sky indicating an overcast day. The camera angle captures her from a straight-on perspective, focusing on her entire body and the surrounding outdoor setting.</p>
	<p>The image captures an indoor setting with stair steps viewed from a slightly elevated angle, focusing on the black metal handrail and the dark stairs below. In the background, a glass railing and the railing's supporting structure are visible, contributing to a modern architectural aesthetic. The lighting is subdued, emphasizing the metallic and glass materials in the scene.</p>
	<p>The image features a religious display set against a richly decorated interior with vertical, multicolored striped curtains and ornate wood paneling. In the foreground, a pedestal supports a statue of Jesus Christ on the cross, flanked by two golden lion-like sculptures with outstretched paws. The camera angle is slightly upward, emphasizing the statue and the intricate details of the backdrop.</p>
	<p>The image displays a dense layer of golden-brown pretzels filling the entire frame, creating a textured background. The foreground is dominated by the uniform, shiny pretzels, shot from a close-up, slightly overhead camera angle that emphasizes their shape and glossiness. There are no other distinct objects or elements visible in the background.</p>
	<p>A rugby match takes place outdoors on a lush green field, with a blurred background of trees indicating a park-like setting. In the foreground, two players are engaged in a tense tackle, with one player wearing a white shirt and gray shorts holding the rugby ball, while the other, in a red and black jersey, attempts to challenge him. The camera angle is slightly tilted and close-up, capturing the intensity of the moment and emphasizing the players' dynamic movements.</p>
	<p>The image features a lush, well-maintained garden area overlooking a body of water, with a few tall palm trees in the background. In the foreground, a traditionally dressed performer with a lei around his neck holds a lit torch or flame, standing on a paved surface. The camera angle captures him at eye level, emphasizing his cultural attire and the scenic outdoor setting behind him.</p>






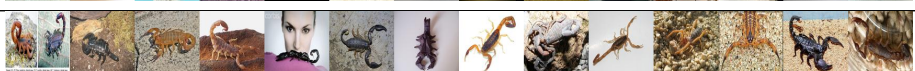
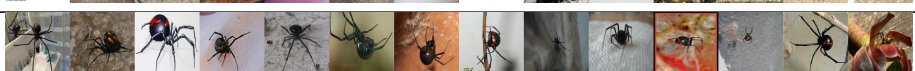
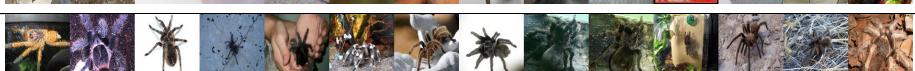

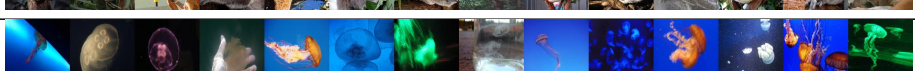
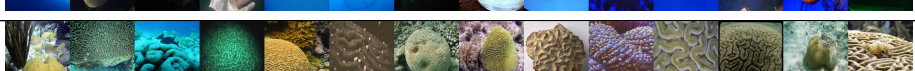
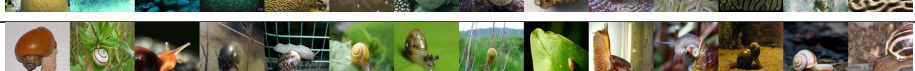
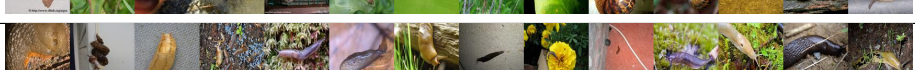
Continued on next page

Table 7 – Continued from previous page

Image	Caption
	<p>The image features a close-up side profile of a golden retriever with a friendly expression, its mouth slightly open and tongue visible. The dog is wearing a collar with a paw print tag and is captured from a slightly lower angle, highlighting its head and upper body. In the background, there is a snowy landscape with trees and falling snowflakes, creating a wintery atmosphere.</p>
	<p>The image depicts a covered porch or veranda with a row of wooden rocking chairs arranged along the railing, facing outward. The background features a misty, foggy landscape with leafless trees, creating a serene and slightly mysterious ambiance. The camera angle is level with the chairs, capturing the perspective of someone standing on the porch looking toward the landscape.</p>
	<p>A young man is sitting on a boat or dock near the water, wearing a bright yellow life jacket. He is smiling and looking toward the camera, with an ocean or large body of water and an overcast sky in the background. The image is taken from a slightly low angle, capturing his upper body and part of his legs, with the water stretching out behind him.</p>
	<p>The image features a close-up view of a fire salamander with striking black and yellow coloration, positioned amidst lush green grass. The camera angle captures the salamander from a top-down perspective, highlighting its elongated body, glossy skin, and distinctive markings. The background consists of dense, vibrant grass blades, providing a natural and contrasting setting for the amphibian.</p>

G. Imagenet-1k Subset

Table 8. We visualize image samples from the subset of the imagenet-1k (200 classes, 500 IPC) that we use as real data in our experiments

Class Name	Sample Images
goldfish	
european fire salamander	
bullfrog	
tailed frog	
american alligator	
boa constrictor	
trilobite	
scorpion	
black widow	
tarantula	
centipede	
goose	
koala	
jellyfish	
brain coral	
snail	
slug	
sea slug	
american lobster	

Continued on next page

Table 8 – Continued from previous page

Class Name	Sample Images
spiny lobster	
black stork	
king penguin	
albatross	
dugong	
chihuahua	
yorkshire terrier	
golden retriever	
labrador retriever	
german shepherd	
standard poodle	
tabby cat	
persian cat	
egyptian cat	
cougar	
lion	
brown bear	
ladybug	
fly	
bee	
grasshopper	

Continued on next page

Table 8 – Continued from previous page

Class Name	Sample Images
walking stick	
cockroach	
mantis	
dragonfly	
monarch	
sulphur butterfly	
sea cucumber	
guinea pig	
hog	
ox	
bison	
bighorn	
gazelle	
arabian camel	
orangutan	
chimpanzee	
baboon	
african elephant	
panda	
abacus	
academic gown	

Continued on next page

Table 8 – Continued from previous page

Class Name	Sample Images
altar	
apron	
backpack	
bannister	
barbershop	
barn	
barrel	
basketball	
bathtub	
beach wagon	
beacon	
beaker	
beer bottle	
bikini	
binoculars	
birdhouse	
bow tie	
brass	
broom	
bucket	
bullet train	

Continued on next page

Table 8 – Continued from previous page

Class Name	Sample Images
butcher shop	
candle	
cannon	
cardigan	
cash machine	
CD player	
chain	
chest	
christmas stocking	
cliff dwelling	
computer keyboard	
confectionery	
convertible	
crane	
dam	
desk	
dining table	
drumstick	
dumbbell	
flagpole	
fountain	

Continued on next page

Table 8 – Continued from previous page

Class Name	Sample Images
freight car	
frying pan	
fur coat	
gasmask	
go-kart	
gondola	
hourglass	
iPod	
jinrikisha	
kimono	
lampshade	
lawn mower	
lifeboat	
limousine	
magnetic compass	
maypole	
military uniform	
miniskirt	
moving van	
nail	
neck brace	

Continued on next page

Table 8 – Continued from previous page

Class Name	Sample Images
obelisk	
oboe	
pipe organ	
parking meter	
pay-phone	
picket fence	
pill bottle	
plunger	
pole	
police van	
poncho	
pop bottle	
potter's wheel	
projectile	
punching bag	
reel	
refrigerator	
remote control	
rocking chair	
rugby ball	
sandal	

Continued on next page

Table 8 – Continued from previous page

Class Name	Sample Images
school bus	
scoreboard	
sewing machine	
snorkel	
sock	
sombrero	
space heater	
spider web	
sports car	
steel arch bridge	
stopwatch	
sunglasses	
suspension bridge	
swimming trunks	
syringe	
teapot	
teddy bear	
thatched roof	
torch	
tractor	
triumphal arch	

Continued on next page

Table 8 – Continued from previous page

Class Name	Sample Images
trolleybus	
turnstile	
umbrella	
vestment	
viaduct	
volleyball	
water jug	
water tower	
wok	
wooden spoon	
comic book	
plate	
guacamole	
ice cream	
lollipop	
pretzel	
mashed potato	
cauliflower	
bell pepper	
mushroom	
orange	

Continued on next page

Table 8 – Continued from previous page

Class Name	Sample Images
lemon	
banana	
pomegranate	
meat loaf	
pizza	
potpie	
espresso	
alp	
cliff	
coral reef	
lakeside	
seashore	
acorn	